energies

MDPI

Communication

NbO_2 as a Noble Zero-Strain Material for Li-Ion Batteries: Electrochemical Redox Behavior in a Nonaqueous Solution

Yang-Soo Kim [1], Yonghoon Cho [2], Paul M. Nogales [2] and Soon-Ki Jeong [2,*]

[1] Jeonju Center, Korea Basic Science Institute, Jeonju 54907, Korea
[2] Department of Energy Systems Engineering, Soonchunhyang University, Soonchunhyang-ro 22-gil, Sinchang-myeon, Asan-si, Chungcheongnam-do 31538, Korea
* Correspondence: hamin611@sch.ac.kr; Tel.: +82-41-530-1313

Received: 11 July 2019; Accepted: 31 July 2019; Published: 1 August 2019

Abstract: Lithium-ion batteries are widely available commercially and attempts to extend the lifetime of these batteries remain necessary. The energy storage characteristics of NbO_2 with a rutile structure as a material for the negative electrode of lithium-ion batteries were investigated. When negative potential was applied to the NbO_2 electrode during application of a constant current in a nonaqueous solution containing lithium ions, these ions were inserted into the NbO_2. Conversely, upon application of positive potential, the inserted lithium ions were extracted from the NbO_2. In situ X-ray diffraction results revealed that the variation in the volume of NbO_2 accompanying the insertion and extraction of lithium was 0.14%, suggesting that NbO_2 is a zero-strain (usually defined by a volume change ratio of 1% or less) active material for lithium-ion batteries. Moreover, the highly stable structure of NbO_2 allows the corresponding electrode to exhibit excellent cycling performance and coulombic efficiency.

Keywords: zero-strain material; NbO_2; negative electrode; lithium-ion battery; energy storage; battery lifetime

1. Introduction

The concept of guest–host electrochemistry has paved the way for the development of secondary batteries [1,2]. In this regard, lithium ions and graphite are widely used as guest and host, respectively, in the negative electrode of commercially available lithium-ion batteries (LIBs), which are considered to be the most advanced type of secondary battery. As the guest lithium ions are inserted (reduced) and extracted (oxidized), energy is stored (charged) and released (discharged), respectively. These electrochemical reactions are generally typified by an increase in the volume of the host during the former process and a decrease during the latter process. However, repeated expansion and contraction of the host electrode material as a consequence of repeated charging and discharging is one of the important causes of battery deterioration.

Therefore, enhanced battery stability requires the volume variation induced by guest ion insertion/extraction of prospective electrode materials to be as small as possible. This means that zero-strain materials, i.e., those featuring negligible volume variation (<1%), are of great importance for the development of long-lifetime rechargeable batteries [3,4]. In addition, a small volume variation would also be expected to suppress damage to the solid electrolyte interphase (SEI) at the electrode–electrolyte interface upon cycling. This would markedly improve the coulombic efficiency because a damaged SEI irreversibly consumes charge during the recovery process [5]. Among others, $Li_4Ti_5O_{12}$ (LTO, volume variation = 0.2%) and $Li_{1+x}Rh_2O_4$ (volume variation = 0.5%) are representative zero-strain materials that have been used to achieve good cycling capability in LIBs [6,7].

LIB electrode materials based on a transition metal oxide exhibit electrochemical redox behavior in the form of either insertion or conversion reactions. The former type accommodates lithium via the insertion of lithium ions into lattice vacancies, whereas the latter type involves alloying reactions between lithium and metal ions to form Li_2O and nano-metal composites [8–10]. Importantly, these two types of materials exhibit large differences in the binding forces between the transition metal and oxygen [11,12]. Among the transition metal oxides, Nb-based oxides have attracted attention as electrode materials with high-energy density owing to a high-tap density [13,14]. In general, Nb-based oxides exist in several different forms such as NbO, NbO_2, Nb_2O_3, and Nb_2O_5 [15]. Among them, very few studies on the properties of NbO_2 as an electrode material for LIB have been reported. Li et al. concluded that lithium ions are electrochemically stored in NbO_2 ~0.9 V vs. Li/Li^+ [12]. However, they did not provide any experimental results to support their conclusion. Cho et al. reported on the charge–discharge characteristics of chemically etched NbO_2 between 0.0 and 3.0 V vs. Li/Li^+, suggesting that the existence of Nb_2O_5 on the surface of NbO_2 affects electrode performance [16]. On the other hand, Park et al. investigated the characteristics of Nb_2O_5/NbO_2 composite electrodes between 1.0 and 3.0 V vs. Li/Li^+, suggesting that the rate performance was improved by NbO_2 [17]. As such, only very limited information on NbO_2 has been reported, and its redox behavior currently remains largely unexplored. This motivated our decision to probe this redox behavior.

At room temperature, NbO_2 has a distorted tetragonal super-structure with a rutile-type sublattice [18]. This structure, illustrated in Figure 1a, is characterized by chains of edge-sharing NbO_6 octahedrons, which are cross-linked by sharing corners where the Nb-O distances in the octahedral are the same. Although the redox mechanism of the electrochemical reaction of NbO_2 with lithium ions is not known, two potential insertion sites with either octahedral or tetrahedral oxygen coordination exist between the octahedra, as shown in Figure 1b [19]. In this study, we investigated the electrochemical redox behavior of NbO_2 between 0.0 and 3.0 V vs. Li/Li^+ in a nonaqueous solution containing lithium ions and discovered this behavior to be different from that reported previously for NbO_2. In addition, we measured the volume variation of this oxide material to demonstrate that it can be viewed as a novel and promising zero-strain material.

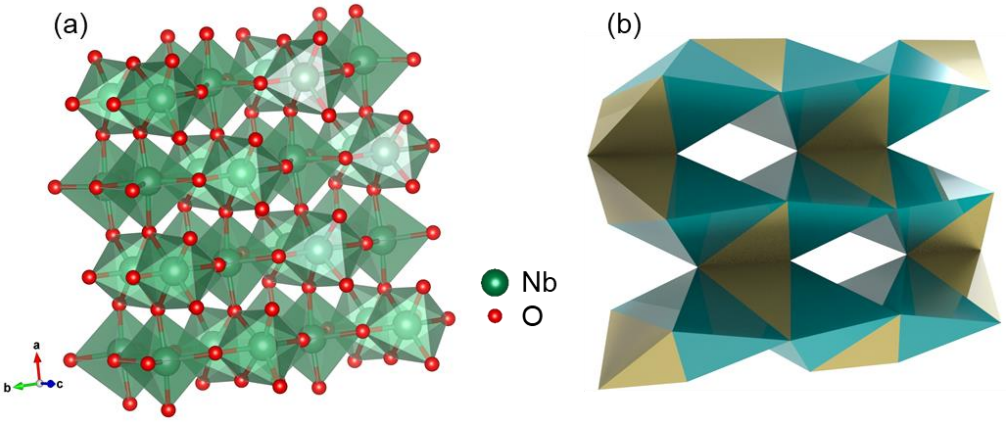

Figure 1. (**a**) Crystal structure of NbO_2 at room temperature and (**b**) expanded view of some octahedral and tetrahedral sites between the octahedra seen in (**a**).

2. Materials and Methods

In situ X-ray diffraction (XRD) was used for the structural analysis of the electrode material using a cell with Kapton windows as described elsewhere [20]. The XRD patterns were collected using a Rigaku MicroMAX 007HF diffractometer with an R-AXIS IV++ image plate using Mo K_α radiation (λ = 0.7107 Å). An electrochemical cell specifically designed for in situ XRD was installed in the diffractometer, connected to a potentiostat (WBCS3000, Wonatech Co., Seoul, Korea), and galvanostatically cycled at 0.05 C while XRD patterns were recorded at intervals of 3 min. To compare

the obtained results with those reported in the literature, 2θ values were converted into those corresponding to Cu K_α radiation (λ = 1.5405 Å).

The working electrode was prepared by coating Cu foil with a mixture of NbO_2 powder (Sigma-Aldrich, 99.9%; 80 wt.%), carbon black (10 wt.%), and poly(vinylidene difluoride) (binder; 10 wt.%) followed by 12-h drying at 100 °C in a vacuum oven. Li foil was used as the counter electrode, and 1 mol dm^{-3} of $LiClO_4$ dissolved in a 1:1 (*v*/*v*) mixture of ethylene carbonate and diethyl carbonate (Panax E-Tec., battery grade) was used as the electrolyte. The working electrode was used to fabricate 2032-type coin cells in an Ar-filled glove box (Three-Shine, SK-G1200) with a dew point below –60 °C. These cells were galvanostatically charged and discharged between 0.0 and 3.0 V using a battery test system (WBCS3000, Wonatech Co., Seoul, Korea). Cyclic voltammetry (CV) measurements were carried out between 0.0 and 3.0 V vs. Li/Li^+ at a sweep rate of 0.5 mV s^{-1}.

3. Results and Discussion

Figure 2 shows the in situ XRD patterns of NbO_2 recorded during constant-current cycling, revealing that all peaks can be indexed to rutile NbO_2 (JCPDS No. 82-1141) and additionally demonstrating the presence of the (111), (200), and (220) planes of Cu (current collector) with reflection peaks at 43.2°, 50.3°, and 73.8°, respectively. Previously, Li et al. reported that NbO_2 electrochemically reacts with lithium via a conversion reaction [12], although no supporting evidence was provided. When used as a negative LIB electrode, Fe_3O_4 was reported to similarly undergo a conversion reaction to afford Li_2O in the first charge cycle, as evidenced by the observation of a Li_2O XRD peak at 33.5° [21]. Likewise, if NbO_2 also underwent a conversion reaction under similar conditions, one would expect to observe the formation of Li_2O at first charge. However, no peaks of Li_2O or other phases are observed in Figure 2a, suggesting that NbO_2 might undergo insertion. In the case of an insertion reaction, lithium ion insertion/extraction would be accompanied by XRD peak shifts to lower/higher angles due to the concomitant expansion/reduction of d-spacing [22]. However, no such peaks shifts were observed during cycling in Figure 2b, indicating that the volume variation in NbO_2 due to lithium insertion/extraction is extremely small.

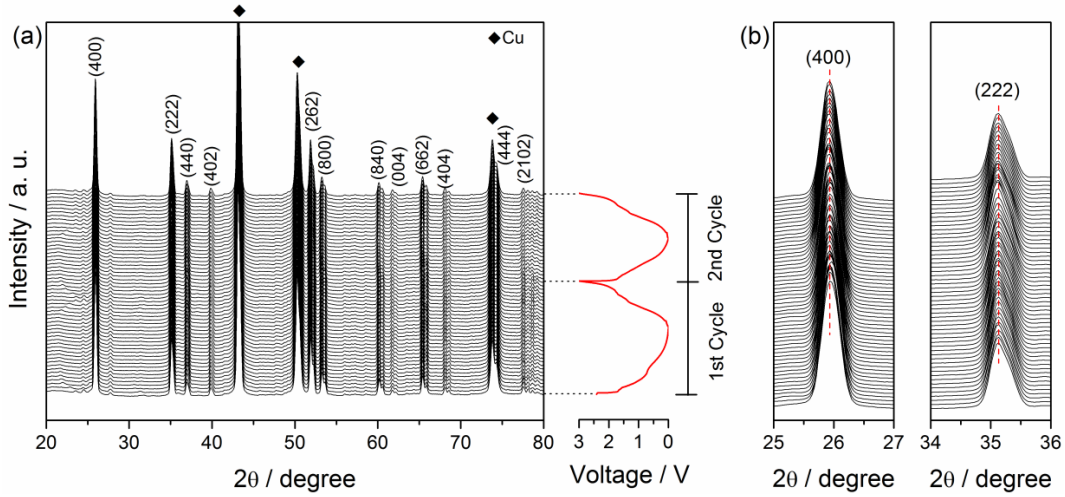

Figure 2. (**a**) In situ X-ray diffraction patterns collected during the charge and discharge of pristine NbO_2 at 0.05 C and (**b**) expansion of the above patterns around the (400) and (222) peaks.

Table 1 presents the lattice parameters (*a*, *b*, *c*) and unit cell volumes (*V*) of NbO_2 calculated from the corresponding XRD patterns using Equations (1) and (2).

$$1/d^2 = (h^2 + k^2)/a^2 + l^2/c^2 \quad (1)$$

$$V = a^2c \quad (2)$$

Table 1. Variation of lattice parameters and volume of pristine NbO_2 during charge and discharge.

State	$a = b$ (Å)	c (Å)	Volume (Å^3)
Pristine	13.7412	6.0037	1133.6
First full charge	13.7528	6.0019	1135.2
First full discharge	13.7413	6.0039	1133.7
Second full charge	13.7526	6.0020	1135.2
Second full discharge	13.7413	6.0040	1133.7

Notably, the lattice parameters and volume determined in the first cycle were slightly different from those determined in the second cycle, probably because the inserted lithium ions could not be completely extracted in the former/latter case. Based on the above data, the volume variation of NbO_2 was calculated as 0.14%, which is smaller than that of LTO (0.2%) as mentioned in the introduction. The electrode material in LIBs in which lithium ions are used as a guest is generally defined as a zero-strain material when the change in the volume of the host induced by charge/discharge cycles accompanied by lithium insertion is within 1%. Therefore, NbO_2 was concluded to be a zero-strain material. Zero-strain materials exhibit excellent cycle characteristics and extend the battery lifetime [3,4].

Figure 3a shows the charge and discharge curves of NbO_2 recorded at 0.05 C (21.4 mA g^{-1}). The presence of an extended plateau at 0.8 V on the first charge curve indicated SEI film formation. The first charge/discharge capacities were determined as 256/152 mAh g^{-1} and corresponded to the insertion/extraction of 1.2/0.7 mol of lithium ions, respectively. The first-cycle irreversible capacity was attributed to electrolyte decomposition and SEI film formation. This is also confirmed by the cyclic voltammograms of the NbO_2 electrode as shown in Figure 3b. In the first cycle, a minor reductive current began to flow at ~1.8 V, and a major reductive peak centered at 0.62 V appeared. This reductive peak, including the minor current between 1.8 and 1.0 V, are absent in the second cycle, indicating that their presence and subsequent disappearance are the result of irreversible electrolyte decomposition, which is closely related to the formation of an SEI. Although the physicochemical correlations between the irreversible electrolyte decomposition and SEI formation are not clear in the present work, there is no doubt about the formation of the SEI on the NbO_2 electrode because the stable charge and discharge reactions shown in Figure 3a would not occur without an SEI. In addition to the small reductive peak, large reductive and oxidative peaks are observed at a potential close to 0 V. These two peaks can be attributed to lithium insertion and extraction events, respectively. Previous studies reported that rutile-structured materials feature two possible sites (with octahedral and tetrahedral coordination environments) for lithium ion insertion [19], whereas Nb-based oxides were reported to undergo a two-electron-transfer reaction with lithium ions [13,14]. Therefore, assuming that rutile-type NbO_2 reacts with two electrons, the insertion/extraction process can be expressed as Equation (3):

$$NbO_2 + 2Li^+ + 2e^- \leftrightarrow Li_2NbO_2 \quad (3)$$

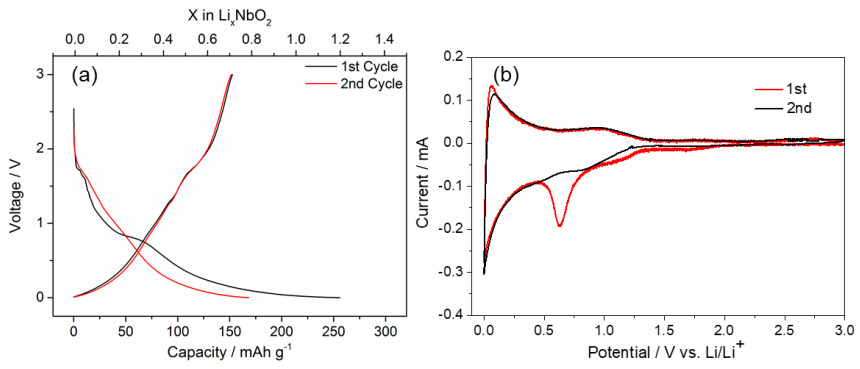

Figure 3. (**a**) Charge and discharge curves and (**b**) cyclic voltammograms of the first and second cycles of pristine NbO_2.

Although the theoretical capacity of NbO_2 (429 mAh g^{-1}) is slightly larger than that of commercial graphite (372 mAh g^{-1}), the former material features a higher tap density (5.9 g cm^{-3}) than the latter (2.2 g cm^{-3}) at room temperature and therefore exhibits a higher volumetric capacity (2531 vs. 833 mAh cm^{-3}). However, the disadvantages of the NbO_2 electrode are its large irreversible capacity and small discharge capacity, which may be caused by the poor electric conductivity (10^{-4} S cm^{-1}) of NbO_2 [23].

Figure 4a shows the cycling performance of NbO_2 at a rate of 1 C (214 mA g^{-1}), demonstrating that the first discharge capacity could be determined as 91 mAh g^{-1} and that a capacity retention of 94% could be observed over 50 cycles. The coulombic efficiency after several initial cycles approached 100% (the low coulombic efficiency during initial cycles was probably caused by SEI film formation upon first charge). Thus, NbO_2 realizes reversible insertion/extraction of lithium ions, exhibits excellent cycling stability, and was therefore concluded to be well suited for use in LIBs, especially considering the additional advantage of being a zero-strain material. As indicated in Figure 4b, the discharge capacities are ~108, ~93, ~74, and ~55 mAh g^{-1} at constant current rates of 0.1, 0.5, 2, and 5 C, respectively. The capacity retention at 5 C is 50.9% of the initial capacity. As the discharge rate increased, the capacity decreased. However, when discharged at 0.1 C after the high rate capability tests, the discharge capacity was almost similar to the initial discharge capacity. This behavior is also observed in LTO, which is a typical zero-strain material [24], and indicates that NbO_2 is structurally highly stable in the process of lithium ion insertion/extraction.

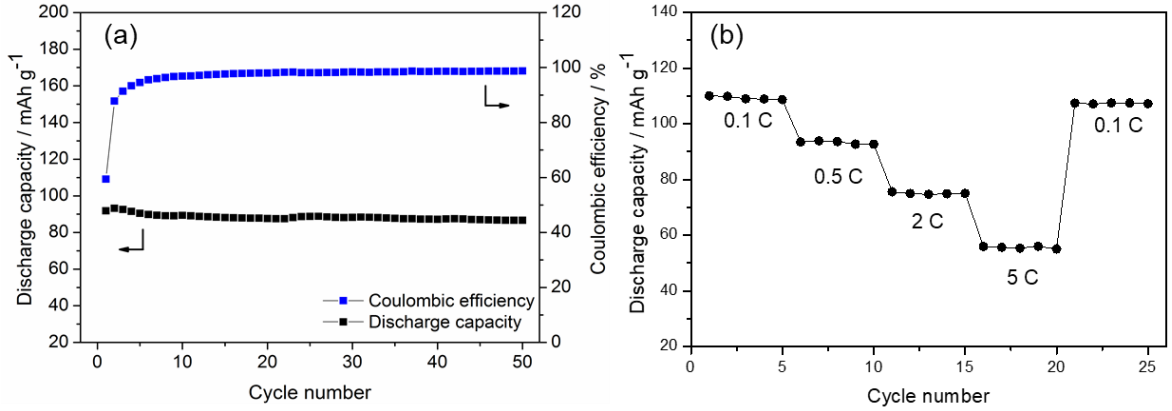

Figure 4. (**a**) Cycling performance and coulombic efficiency determined at 1 C and (**b**) rate capabilities of pristine NbO_2.

4. Conclusions

In this study, we investigated the electrochemical redox reactions of NbO_2 as a negative electrode material for LIBs. In contrast to the results of previous studies, NbO_2 was shown to react with lithium ions via an insertion reaction and to exhibit an ultra-low volume variation of 0.14%. The small magnitude of the above volume change allowed the integrity of the entire crystal structure to be well preserved during cycling and resulted in impressive cycling stability and coulombic efficiency. However, the observed capacity was much lower than the theoretically predicted value, which was ascribed to poor electric conductivity. Therefore, further work on conductivity improvement is needed to render NbO_2 a promising negative electrode for LIBs. In this regard, carbon coating of the NbO_2 particles may be the most effective and low-cost approach, because it would improve the surface electronic conductivity and electrical contact with the electrolyte solution. In addition, doping with metal ions, hybridization with metal powder, and reduction of the particle size could be considered as possible strategies for improving the electric conductivity. Additional studies to overcome the low electric conductivity are currently underway.

Author Contributions: Conceptualization, Y.-S.K. and S.-K.J.; methodology, Y.C. and P.M.N.; formal analysis, Y.-S.K. and S.-K.J.; investigation, Y.C. and P.M.N.; resources, Y.C.; data curation, Y.C.; writing—original draft preparation, Y.-S.K. and S.-K.J.; writing—review and editing, S.-K.J.; supervision, S.-K.J.; project administration, S.-K.J.; funding acquisition, S.-K.J.

Funding: This research was funded by the Korea Institute of Energy Technology Evaluation and Planning (KETEP) and the Ministry of Trade, Industry & Energy (MOTIE) of the Republic of Korea (No. 20184030202130).

Acknowledgments: This work was also supported by the Soonchunhyang University Research Fund.

Conflicts of Interest: The authors declare no conflict of interest.

References

1. Armand, M.; Tarascon, J.-M. Building better batteries. *Nature* **2008**, *451*, 652–657. [CrossRef] [PubMed]
2. Winter, M.; Besenhard, J.O.; Spahr, M.E.; Novak, P. Insertion electrode materials for rechargeable lithium batteries. *Adv. Mater.* **1998**, *10*, 725–763. [CrossRef]
3. Lu, X.; Zhao, L.; He, X.; Xiao, R.; Gu, L.; Hu, Y.-S.; Li, H.; Wang, Z.; Duan, X.; Chen, L.; et al. Lithium storage in $Li_4Ti_5O_{12}$ Spinel: The full static picture from electron microscopy. *Adv. Mater.* **2012**, *24*, 3233–3238. [CrossRef] [PubMed]
4. Ohzuku, T.; Ueda, A.; Yamamota, N. Zero-strain insertion material of Li $[Li_{1/3}Ti_{5/3}]O_4$ for rechargeable lithium cells. *J. Electrochem. Soc.* **1995**, *142*, 1431–1435. [CrossRef]
5. You, Y.; Wu, X.-L.; Yin, Y.-X.; Guo, Y.-G. A zero-strain insertion cathode material of nickel ferricyanide for sodium-ion batteries. *J. Mater. Chem. A* **2013**, *1*, 14061–14065. [CrossRef]
6. Zhao, L.; Hu, Y.-S.; Li, H.; Wang, Z.; Chen, L. Porous $Li_4Ti_5O_{12}$ coated with N-doped carbon from ionic liquids for Li-ion batteries. *Adv. Mater.* **2011**, *23*, 1385–1388. [CrossRef] [PubMed]
7. Gu, Y.; Taniguchi, K.; Tajima, R.; Nishimura, S.-I.; Hashizume, D.; Yamadac, A.; Takagi, H. A new "zero-strain" material for electrochemical lithium insertion. *J. Mater. Chem. A* **2013**, *1*, 6550–6552. [CrossRef]
8. Poizot, P.; Laruelle, S.; Grugeon, S.; Dupont, L.; Tarascon, J.-M. Nano-sized transition-metal oxides as negative-electrode materials for lithium-ion batteries. *Nature* **2000**, *407*, 496–499. [CrossRef] [PubMed]
9. Ohzuku, T.; Kodama, T.; Hirai, T. Electrochemistry of anatase titanium dioxide in lithium nonaqueous cells. *J. Power Sources* **1985**, *14*, 153–166. [CrossRef]
10. Liaw, B.Y.; Raistrick, I.D.; Huggins, R.A. Thermodynamic and structural considerations of insertion reactions in lithium vanadium bronze structures. *Solid State Ion.* **1991**, *45*, 323–328. [CrossRef]
11. Ku, J.H.; Jung, Y.S.; Lee, K.T.; Kim, C.H.; Oh, S.M. Thermoelectrochemically activated MoO_2 powder electrode for lithium secondary batteries. *J. Electrochem. Soc.* **2009**, *156*, A688–A693. [CrossRef]
12. Li, H.; Balaya, P.; Maier, J. Li-storage via heterogeneous reaction in selected binary metal fluorides and oxides. *J. Electrochem. Soc.* **2004**, *151*, A1878–A1885. [CrossRef]
13. Wei, M.; Wei, K.; Ichihara, M.; Zhou, H. Nb_2O_5 nanobelts: A lithium intercalation host with large capacity and high rate capability. *Electrochem. Commun.* **2008**, *10*, 980–983. [CrossRef]
14. Jian, Z.; Lu, X.; Fang, Z.; Hu, Y.-S.; Zhou, J.; Chen, W.; Chen, L. $LiNb_3O_8$ as a novel anode material for lithium-ion batteries. *Electrochem. Commun.* **2011**, *13*, 1127–1130. [CrossRef]
15. Nowak, I.; Ziolek, M. Niobium compounds: Preparation, characterization, and application in heterogeneous catalysis. *Chem. Rev.* **1999**, *99*, 3603–3624. [CrossRef] [PubMed]
16. Cho, Y.; Jeong, S.-K.; Kim, Y.-S. Electrochemical properties of chemically etched-NbO_2 as a negative electrode material for lithium ion batteries. *Adv. Mater. Res.* **2015**, *1120*, 115–118. [CrossRef]
17. Park, H.; Lee, D.; Song, T. High capacity monoclinic Nb_2O_5 and semiconducting NbO_2 composite as high-power anode material for Li-Ion batteries. *J. Power Sources* **2019**, *414*, 377–382. [CrossRef]
18. Nico, C.; Monteiro, T.; Graça, M.P.F. Niobium oxides and niobates physical properties: Review and prospects. *Prog. Mater. Sci.* **2016**, *80*, 1–37. [CrossRef]
19. Koudriachova, M.V.; Harrison, N.M.; de Leeuw, S.W. Diffusion of Li-ions in rutile. An ab initio study. *Solid State Ion.* **2003**, *157*, 35–38. [CrossRef]
20. Shin, H.C.; Park, S.B.; Jang, H.; Chung, K.Y.; Cho, W.I.; Kim, C.S.; Cho, B.W. Rate performance and structural change of Cr-doped $LiFePO_4$/C during cycling. *Electrochim. Acta* **2008**, *53*, 7946–7951. [CrossRef]
21. Zhang, Q.; Shi, Z.; Deng, Y.; Zheng, J.; Liu, G.; Chen, G. Hollow Fe_3O_4/C spheres as superior lithium storage materials. *J. Power Sources* **2012**, *197*, 305–309. [CrossRef]

22. Ku, J.W.; Park, K.; Ryu, J.H.; Oh, S.M. Electrochemical characteristics of $Li_3V_2(PO_4)_3$ negative electrode as a function of crystallinity. *J. Korean Electrochem. Soc.* **2012**, *15*, 27–34. [CrossRef]
23. Adler, D. Mechanisms for metal-nonmental transitions in transition-metal oxides and sulfides. *Rev. Mod. Phys.* **1968**, *40*, 714–736. [CrossRef]
24. Chang, C.-M.; Chen, Y.-C.; Ma, W.-L.; Chen-Yang, Y.W. High rate capabilities of $Li_4Ti_{5-x}V_xO_{12}$ ($0 \leq x \leq 0.3$) anode materials prepared by a sol–gel method for use in power lithium ion batteries. *RSC Adv.* **2015**, *5*, 49248–49256. [CrossRef]

© 2019 by the authors. Licensee MDPI, Basel, Switzerland. This article is an open access article distributed under the terms and conditions of the Creative Commons Attribution (CC BY) license (http://creativecommons.org/licenses/by/4.0/).